Alterations in the blood brain barrier in ageing cerebral cortex in relationship to Alzheimer-type pathology: A study in the MRC-CFAS population neuropathology cohort

Andrew P. Viggars [a,1], Stephen B. Wharton [a,*,1], Julie E. Simpson [a,1], Fiona E. Matthews [b,1], Carol Brayne [c,1], George M. Savva [d,1], Claire Garwood [a,1], David Drew [a,1], Pamela J. Shaw [a,1], Paul G. Ince [a,1]

[a] Sheffield Institute for Translational Neuroscience, University of Sheffield, 385A Glossop Road, Sheffield S10 2HQ, UK
[b] MRC Biostatistics Unit, University of Cambridge, UK
[c] Department of Public Health and Primary Care, Institute of Public Health, University of Cambridge, UK
[d] Department of Medical Gerontology, Trinity College, Dublin, Ireland

ARTICLE INFO

ABSTRACT

Impairment of the blood brain barrier (BBB) in human brain ageing and its relationship to Alzheimer-type pathology remains poorly defined. We have investigated the BBB in temporal cortex of brain donations from a population-representative sample of 92 participants from the Medical Research Council Cognitive Function and Ageing Study (MRC CFAS), a longitudinal study with a programme of brain donation. BBB alteration was investigated by immunohistochemistry to albumin and fibrinogen and to the tight junction proteins claudin-5, zonula occludens-1 (ZO-1) and occludin. BBB leakage showed wide population-variation and increased with progression of Alzheimer-type pathology, though with considerable overlap between different levels of Alzheimer-type pathology. This was accompanied by increased mean vascular density, but not by down-regulation of tight junction proteins. ZO-1 and occludin were also expressed in glia. Mechanisms leading to BBB leakage in brain ageing remain to be defined, but the population-variation in BBB changes and its early increase in relationship to Alzheimer-type pathology progression suggest that BBB dysfunction contributes to brain ageing.

The blood brain barrier (BBB) resides at the endothelium, but the neurovascular unit, a functional association of neurons, astrocytes and microvasculature, is important in its integrity. Tight junction protein (TJP) complexes, an important structural component of the BBB, consist of transmembrane proteins, including claudins and occludin, that form the barrier between endothelial cells, and accessory proteins, such as the zonula occludens family [33,35].

BBB disruption occurs in various neurological disorders, including trauma, ischaemia [19,26], neurodegeneration and inflammatory disorders such as multiple sclerosis and HIV encephalitis [1,6,11,35]. BBB dysfunction is associated with TJP down-regulation and leakage of plasma proteins. Pathological and imaging studies suggest that BBB dysfunction occurs in Alzheimer's disease (AD) and may contribute to its development through impaired Aβ-peptide clearance and neuroinflammation [24,34,35].

A systematic review has shown that BBB dysfunction increases in brain ageing and in Alzheimer's and vascular dementias, but study findings have varied, indicating that further investigation is needed [7]. We [29], and others [7] have shown BBB dysfunction in white matter lesions, which contribute to dementia in the population. Therefore, defining cortical changes in the BBB in ageing is an important question.

This study used well-characterised cases from the neuropathology cohort of the Medical Research Council Cognitive Function and Ageing Study (CFAS). CFAS is a population-representative longitudinal study of cognitive impairment and frailty in older (>65 y) people, which represents a continuum of brain ageing [16,18]. Overlap in burdens of Alzheimer-type lesions between demented and non-demented individuals in this cohort implies a role for non-classical markers. BBB dysfunction is one such candidate process. We therefore investigated variation in the BBB in the elderly human (temporal) cortex and the relationship to Alzheimer-type pathology.

Autopsy brains from a single CFAS centre (Cambridge) were used, thereby maintaining the population-representative nature of the cohort. This consisted of 92 well-characterised cases, previously

* Corresponding author. Tel.: +44 0114 222 2261.
  E-mail address: s.wharton@sheffield.ac.uk (S.B. Wharton).
[1] On behalf of the MRC Cognitive Function and Ageing Study Neuropathology Group.

described [28]. Informed consent for all participants and ethics committee approval were obtained. For each case, one hemisphere was formalin-fixed prior to sampling, within 4–6 weeks, into paraffin blocks. The other hemi-brain was sliced, flash-frozen in liquid nitrogen and stored at $-80\,^\circ C$. Cases were previously staged for Alzheimer-type pathology using CERAD [17] and Braak [4] schemes. Analyses were performed in relation to pathological features, rather than to pre-defined diagnostic categories, but, for information, the cohort included 8 cases satisfying CERAD criteria for AD, 14 for probable-AD and 20 possible-AD. Braak staging was determined by AT8 immunostaining [3]. 28 cases were entorhinal stages (I–II), 47 limbic (III–IV) and 17 isocortical (VI). Assessment was performed blind to clinico-pathological information. The study focused on the lateral temporal neocortex. Tangles and plaques were quantified as none, mild, moderate and severe.

Immunohistochemistry for claudin-5, collagen-IV, albumin and fibrinogen was performed on formalin-fixed paraffin-embedded tissue sectioned at 5 μm. A standard avidin–biotin complex (ABC) method (Vector Laboratories, UK) was used and the signal visualised by diaminobenzidine (DAB). Negative controls consisted of sections incubated with isotype controls or in the absence of primary antibody (Table 1). Double-staining experiments were performed for albumin and GFAP using a combined colour product and fluorescence method [28]. Briefly, albumin expression was visualised as above, and incubated with the avidin–biotin blocking kit (Vector Laboratories, UK) as per manufacturer's instructions. Sections were then incubated with anti-GFAP (DakoCytomation, UK) at 1:500 overnight at $4\,^\circ C$, followed by biotinylated secondary antibody, then with Streptavidin TRITC (Serotec, UK) in the dark for 1 h at I:100, RT. Image capture was performed using CellR̂ Software (Olympus Biosystems, Watford, UK).

As antibodies to zonula occludens-1 (ZO-1) and occludin did not demonstrate signal in formalin-fixed material, we studied their expression in frozen sections of the contralateral temporal cortex from a sub-cohort, selected from the 3 Braak groups by colleagues at the MRC biostatistics unit (GS and FM), to ensure that they remained representative. Of those selected, suitable quality preparations were obtained from 28 cases; 10 from entorhinal, 11 from limbic and 7 from isocortical stage cases. Frozen sections (7 μm) were fixed in cold acetone for 10 min and blocked with normal serum prior to application of the primary antibody (Table 1). Bound antibody was detected using the ABC method with DAB.

Frozen tissue from 7 entorhinal and 7 isocortical cases was homogenised in suspension buffer (10 mM Tris–HCl (pH 7.4), 1 mM ethylene glycol tetraacetic acid, 0.8 M sodium chloride, 10% (w/v) sucrose and 0.1 mM phenylmethanesulfonylfluoride). Homogenates were centrifuged at 14,000 rpm for 30 min at $4\,^\circ C$ and supernatants retained. Protein concentration was determined using a BCA protein assay (Pierce Endogen, Rockford, USA) and samples were standardized to equal protein concentration prior to SDS-PAGE. 15 μg of protein was loaded and separated on 12% (w/v) SDS-PAGE gels and electrophoretically transferred to nitrocellulose membranes. Membranes were incubated in 5% (w/v) non-fat dried milk for 30 min prior to incubation in claudin-5 monoclonal antibody (mouse monoclonal; Dako Ltd., Ely, UK) overnight at $4\,^\circ C$. Following washes membranes were incubated with HRP-coupled secondary antibody (Dako Ltd.) for 1 h at ambient temperature and immunoreactive species visualised using EZ-ECL development reagents (Biological Industries, Israel) and detection carried out by the G:Box Chemi-XT CCD Gel imaging system (Syngene, Cambridge, UK). Membranes were probed with a monoclonal antibody against GAPDH to ensure equal protein loading and bands quantified by densitometric analysis.

Albumin and fibrinogen were scored semi-quantitatively in the most strongly reactive area. Neuropil reactivity was scored as none (1), patchy (2) or confluent (3). Astrocyte expression was assessed in cortical layers II–VI as none (1), isolated (2), frequent (3) or very frequent (4). Astrocyte expression in subpial layer I was not assessed as it was similar across the cohort. Expression in neuronal cytoplasm was assessed as none (1), isolated (2), frequent, representing up to approximately 50% of neurons (3), or very frequent, representing more than 50% (4). Scores in the three domains were summed to give a total out of 11. A photomicrograph composite was produced to assist consistency of scoring (Supplementary Fig. 1). Sections were scored independently by two observers, blind to Alzheimer-type pathology. Total scores agreed in 23.7% and 26.9% of cases or were discrepant by only 1 or 2 marks in 47.3% and 61.2% for albumin and fibrinogen respectively. Good correlation between the 2 observers (Spearman's, $p < 0.001$ for albumin and fibrinogen), indicated that both observers ranked cases in a similar way.

Quantification of claudin-5 and collagen-IV was performed in bright-field microscopic images, captured using a $20\times$ objective (Olympus Cell-R, Olympus Biosystems, UK) in 3 adjacent cortical ribbons from outer cortex to white matter border. Images were thresholded and the area of immunoreactivity measured as a percentage of the total field area, using Image Pro Plus v4.5.1 software (Media Cybernetics, Bethesda, USA). For ZO-1, the percentage of vessels showing an abnormal staining pattern was assessed [11,13]. Approximately 30 vessels per case were imaged and each scored by 2 observers as either normal, with continuous bands of interendothelial cell staining, or abnormal, with areas of broken staining.

Statistical analyses were carried out using PASW Statistics 18 (SPSS Inc). Correlation was measured using Spearman's rank correlation coefficient. Levels of protein expression were described by median and inter-quartile range. TJP expressions were compared between Braak groups, and plaque and tangle groups using the Kruskal–Wallis (K–W) test, and trends across groups assessed by the Jonkheere–Terpstra (J–T) test. Mann–Whitney with Bonferroni correction was used for post hoc testing. For correlations, all Braak stages (0–6) were used, while for between-group comparisons, Braak stages were combined into entorhinal (0–II), limbic (III–IV) and isocortical (V–VI) groups. When comparing across groups defined by tangles and plaques, moderate and severe score groups were combined because of small numbers with severe scores.

Reactivity for albumin and fibrinogen was variably observed in neuropil, neuronal cell bodies and astrocytes (Fig. 1A–F, Supplementary Fig. 1). Neurons were recognised by their pyramidal morphology. Astrocyte uptake for albumin was confirmed by double-labelling for GFAP (Fig. 1D–F). Progression of Alzheimer-type pathology, assessed by Braak stage, was associated with increasing albumin ($r = 0.22$, $p = 0.038$) and fibrinogen ($r = 0.31$, $p = 0.11$) extravasation, reflected by patchy-to-confluent neuropil immunoreactivity and increased immunoreactive neurons and astrocytes. Albumin and fibrinogen immunoreactivities varied with temporal cortex tangle score ($p = 0.028$ and 0.057 respectively) with trend analysis showing more tangles associated with higher albumin ($p = 0.012$) and fibrinogen ($p = 0.023$) scores. Fibrinogen score varied significantly between neuritic plaque groups ($p = 0.028$) but not diffuse plaque groups, although trend analysis showed that fibrinogen score increased with both neuritic ($p = 0.01$) and diffuse plaque ($p = 0.038$) scores (Fig. 2A–C). Albumin-reactivity did not show a significant relationship to plaques.

Claudin-5 reactivity showed diffuse reactivity, confined to endothelium (Fig. 1G), whereas ZO-1 stained linear profiles in capillaries, representing tight-junctions between endothelial cells (Fig. 1I,J). Abnormalities of ZO-1 staining were subtle, consisting of focal areas of staining loss, observable at high-power (Fig. 1K). Reactivity of glial cells for ZO-1 occurred uncommonly. Occludin reactivity was seen in vessels and also in glia (Fig. 1L), so quantification of vessel-associated occludin expression was not attempted.

Table 1
Antibody sources and conditions.

Antibody	Tissue	Isotype	Dilution (time, temp)	Antigen retrieval	Supplier
Claudin-5	FFPE	Mouse IgG	1:100 (o/n, 4 °C)	PC, EDTA pH 8.0	Zymed
Collagen-IV	FFPE	Mouse IgG	1:100 (o/n 4 °C)	MW 15 min, TSC pH 6.5	Sigma
Albumin	FFPE	Rabbit IgG	1:16,000 (1 h RT)	MW 10 min TSC pH 6.5	DakoCytomation
Fibrinogen	FFPE	Rabbit IgG	1:4000 (1 h RT)	MW 10 min TSC pH 6.5	Alere Ltd.
Claudin-5	Frozen	Mouse IgG	1:100 (1 h RT)	–	Zymed
ZO-1	Frozen	Rabbit IgG	1:100 (1 h RT)	–	Zymed
Occludin	Frozen	Rabbit IgG	1:100 (1 h RT)	–	Zymed

FFPE: formalin fixed paraffin embedded, o/n: overnight, RT: room temperature, PC: pressure cooker, MW: microwave, TSC: tri-sodium citrate.
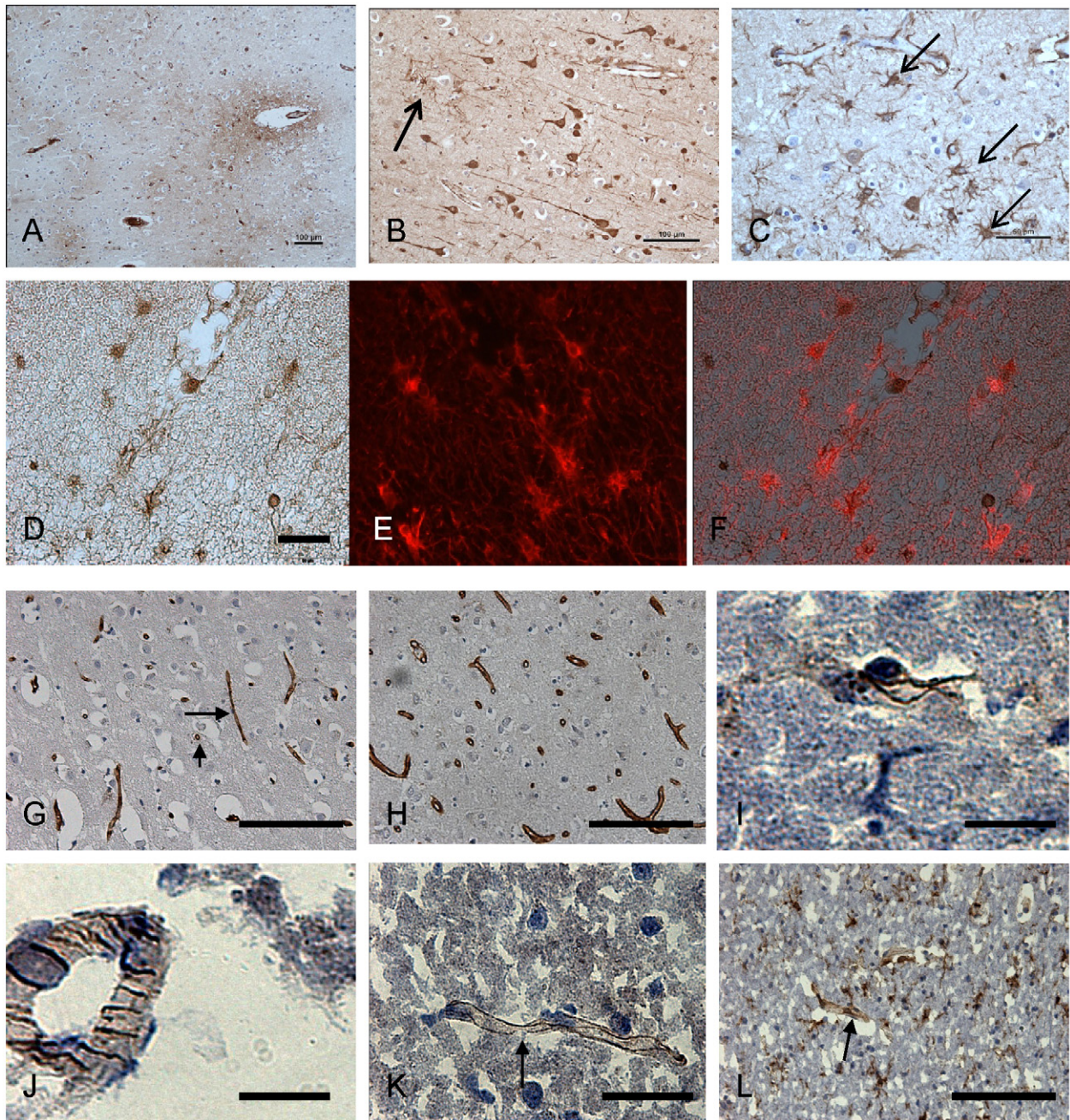

Fig. 1. (A) Patchy parenchymal reactivity, some perivascular, for fibrinogen. (B) Frequent fibrinogen-reactive neurons; astrocytes also present (arrow). (C) Fibrinogen-reactive astrocytes (arrows). (D–F) Double-labelling showing immunoreactivity for albumin in astrocytes; (C) albumin visualised with DAB under light microscopy, (D) astrocytes with GFAP-fluorescent label, (E) superimposed images showing co-localisation of albumin and GFAP. (G) Capillaries labelled for claudin-5. (H) Capillaries outlined by immunohistochemistry to collagen-IV. (I, J) Immunohistochemistry to ZO-1 showing localisation at endothelial cell borders of blood vessels. (J) Abnormal pattern of ZO-1 showing a gap in linear reactivity (arrow). (K) Occludin immunohistochemistry showing reactivity on blood vessels and parenchymal glial cells. Magnification bars: A, B – 100 μm, G, L – 200 μm; C–F, H–K – 50 μm.

Table 2
Quantitation of tight junction proteins and microvessel measures.

Braak group (stages)	(1) Entorhinal (0–II)	(2) Limbic (III–IV)	(3) Isocortical (V–VI)
Claudin-5[a]	0.66 (0.5–.09)	0.73 (0.6–0.9)	0.83 (0.7–1.2)
Collagen-IV[a]	0.82 (0.6–1.0)	0.95 (0.8–1.2)	1.32 (0.9–1.7)
Claudin:collagen[a]	0.95 (0.6–1.2)	0.77 (0.5–1.1)	0.74 (0.5–1.0)
Microvessel density[b]	23.84 (19.5–27.4)	24.32 (20.4–28.4)	26.42 (23.8–33.7)
Inter-vessel distance[c]	150.9 (132–162)	148.2 (131–155)	141.4 (124–156)
ZO-1%abnormal vessels	80.00 (72.5–83.3)	76.66 (66.7–90.0)	76.66 (73.3–83.3)

Values are median (interquartile range).
[a] % area reactivity.
[b] Microvascular density.
[c] Average nearest neighbour pixel distance.

Area-immunoreactivity for claudin-5 did not change with Braak Group (Table 2). To control for the number of microvessels, we assessed microvessels by area-immunoreactivity for collagen-IV and calculated the claudin-5 to collagen-IV ratio. Collagen-IV area-immunoreactivity (Fig. 1H) varied between Braak groups ($p = 0.002$), with a trend to increase with Braak group progression ($p = 0.001$, Fig. 2D). Post hoc testing showed that collagen-IV increased from the limbic to isocortical Braak stages ($p = 0.018$). Collagen-IV also increased with local tangle score ($p = 0.047$) but not with neuritic plaques. Claudin-5 to collagen-IV ratios did not change with Alzheimer-type pathology (Fig. 2D).

Brain homogenates from entorhinal and isocortical Braak groups were probed with an antibody against claudin-5, which showed a band of the expected molecular weight. Within each group large variations in the level of claudin-5 were detected but there was no evident change in claudin-5 expression between Braak groups (Fig. 2E).
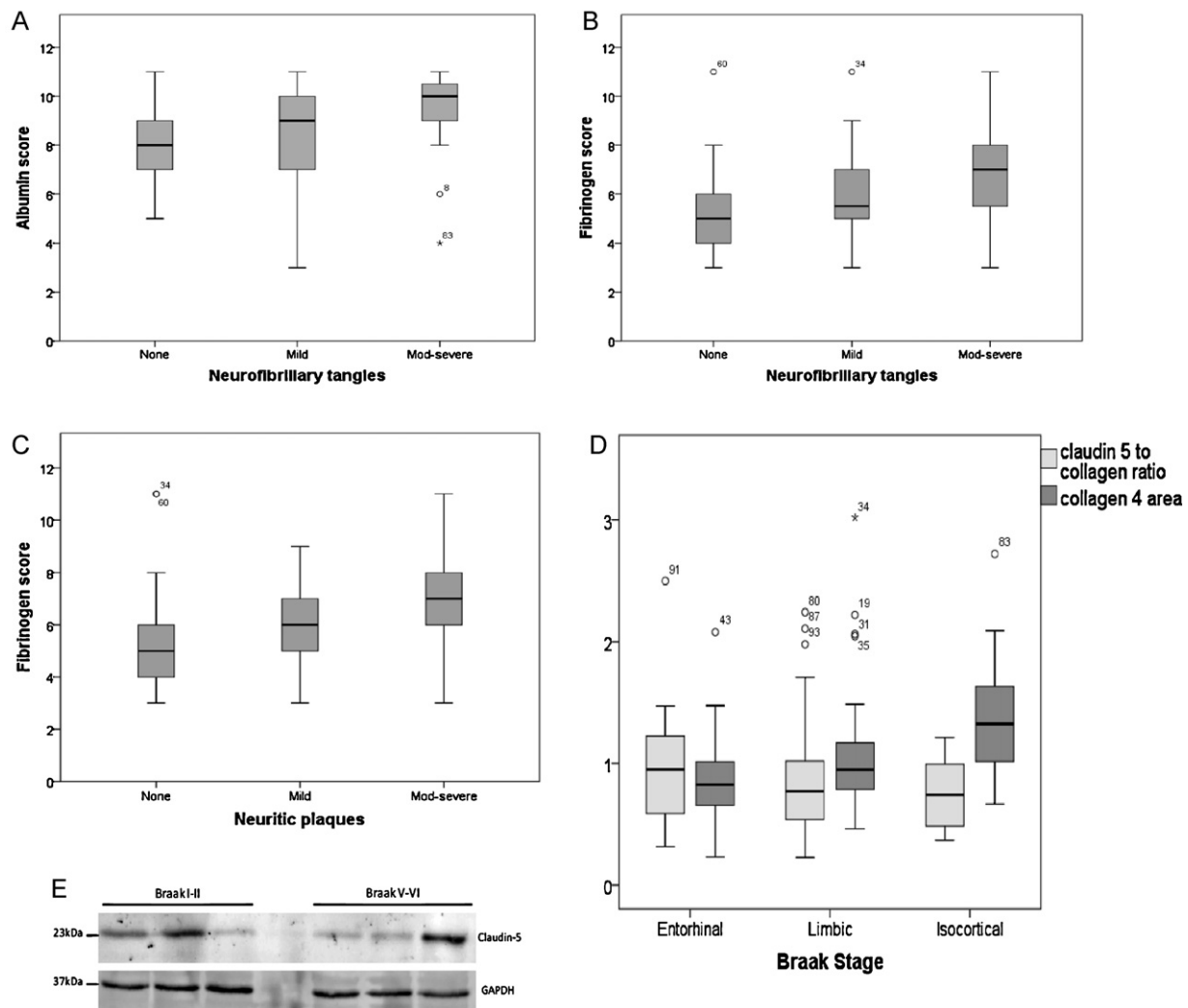

Fig. 2. Box plots showing plasma marker scores compared to Alzheimer-type pathologies; (A) albumin and tangle scores; (B) fibrinogen and tangle scores; (C) fibrinogen and neuritic plaque scores. Outliers >1.5× interquartile range from the upper or lower margin of the box. (D) Area immunoreactivity for collagen-IV and claudin:collagen for entorhinal, limbic and isocortical Braak stages. (E) Representative western blot of homogenates showing variation in claudin-5 at entorhinal and isocortical Braak stages. Blots were probed with an antibody against claudin-5 (23 kDa), GAPDH (37 kDa) was used as loading control. Molecular weight markers are indicated (kDa).

To further assess the change in collagen-IV with ATP progression, we measured the microvascular density (MVD) and the average inter-vessel pixel distance using the collagen-IV preparations (Table 2). There was a difference in MVD ($p = 0.025$), which increased with Braak group ($p = 0.023$), but not inter-pixel distance. As for area-immunoreactivity, post hoc testing demonstrated that MVD increased particularly from limbic to isocortical Braak groups ($p = 0.048$). Thus, collagen-IV area immunoreactivity increased with ATP progression due to an increased MVD, particularly with progression from limbic to isocortical Braak groups. ZO-1 showed no variation between Braak groups ($p = 0.87$), nor was there a trend to change ($p = 0.75$). Neither albumin nor fibrinogen showed a correlation with measures of TJP.

We here show that BBB leakage increases in the ageing cortex with the degree of Alzheimer-type pathology, assessed by Braak stage, and with local tangle and (for fibrinogen) plaque scores. There was considerable population-variation at all Braak stages, with overlap between stages. BBB leakage is therefore not confined to established AD, but occurs in some individuals with little Alzheimer-type pathology, suggesting that BBB dysfunction may occur early in AD progression, or be an independent contributor to ageing brain pathology. The analyses in this study were in relation to burdens of pathology as part of a population-based assessment, and not in relation to clinical phenotypes.

That BBB dysfunction occurs "early" in the development of AD is supported by imaging studies [31], although its assessment in life or in autopsy tissue is difficult. BBB changes precede plaque formation in transgenic models [32]. This parallels findings for oxidative stress, markers of which are also elevated in some individuals with little Alzheimer-type pathology and appear "early" in relation to Alzheimer-type pathology [20–22,27]. Oxidative stress can affect the BBB, causing TJP down-regulation [12] and may cause BBB compromise. Early Alzheimer-related molecular pathologies may also be important; soluble Aβ-aggregates enhance permeability of brain endothelial-cell monolayers [8]. The pathogenic interaction between these factors remains to be determined, but changes in the neurovascular unit appear to be important in ageing, in early AD, and they may contribute to cognitive impairment [24].

The relationship of BBB damage to vascular pathology is an important question. Albumin and fibrinogen did not show a relationship to local microinfarcts in temporal cortex in this study (present in 6% of cases; data not shown), but a comprehensive investigation of brain BBB alterations to the wide range of potential vascular pathologies and to white matter lesions is beyond the scope of this report and is a limitation of the present study.

Fibrinogen and albumin immunoreactivity in neurons and astrocytes implies up-take of the extravasated protein. Uptake of plasma proteins by neurons has been reported following ischaemia [14]. In white matter, astrocytes take up fibrinogen following BBB dysfunction, adopting "clasmatodendritic" morphology [30], implying that uptake of plasma proteins is associated with a cellular pathology. Astrocytes, as a key component of the neurovascular unit [1], may be affected by changes of the BBB.

Reduced TJP-expression has been associated with BBB dysfunction in a number of disorders [6,11,19,26,33]. In this study, we did not demonstrate significant changes in TJP in relation to Alzheimer-type pathology, nor did their expression correlate with plasma-protein leakage. Our methods may be insufficiently sensitive, although similar methods have been used in human autopsy tissue in other disorders [11,13]. Assessment of ZO-1 particularly should be considered as limited, given the number of vessels assessed and high variability in our hands. A second possibility is that such changes are transient. In multiple sclerosis, TJP changes are persistent [13], although the inflammatory cell infiltration here may be associated with greater change to the BBB. In a BBB culture-model, increased paracellular permeability has been

shown without TJP loss [9]. Other potential mechanisms for BBB alterations, such as caveolae, transendothelial channel formation [19] and molecular alterations to TJP, such as phosphorylation [33], would be worth investigating.

A further finding was the increase in microvascular density with increasing Alzheimer-type pathology, particularly from limbic to isocortical tangle stages. This is at variance with some other studies showing a decrease in microvessels in ageing and AD, possibly reflecting capillary loss (reviewed in [5]). Factors such as synaptic loss with AD progression may affect vascular density and the population-basis of our cohort will have resulted in more intermediate stages of AD-progression being examined than in case–control studies, where case selection can result in extremes of disease versus normality. There may also be variation between brain regions. Mann et al. found that measures of capillaries decreased with ageing in frontal but not temporal cortex [15]. Our results do not preclude endothelial damage and collapse, a substrate for BBB-leakage [5], with Alzheimer's pathology progression in our cohort.

ZO-1 and occludin were both expressed by glia. We have also demonstrated ZO-1 and occludin, but not claudin in astrocyte cultures (additional data, Supplementary Fig. 2). Neuronal and glial expression of ZO-1 and occludin has been demonstrated *in vivo* in neuropathological studies [25,29] and *in vitro* [2,10]. TJP may have other roles in glia. Their co-localisation with connexins and the transcription factor MsY3 implies roles in signalling and transcription modulation [23], implying wider roles across glial networks that may be perturbed in ageing and neurodegeneration.

This study provides evidence for BBB leakage in brain ageing which progresses with severity of Alzheimer-type pathology, but which is seen at early stages, suggesting that it may be a useful therapeutic target. Assessment of the BBB remains difficult, and there remains a need for better techniques to define BBB alterations in human tissue. The constellation of BBB dysfunction – oxidative stress – inflammation is important to define as a potential contributor to cerebral dysfunction in ageing.

Acknowledgements

Appendix A. Supplementary data

Supplementary data associated with this article can be found, in the online version, at doi:10.1016/j.neulet.2011.09.049.

References

[1] N. Abbott, L. Ronnback, E. Hansson, Astrocyte–endothelial interactions at the blood–brain barrier, Nat. Rev. Neurosci. 7 (2006) 41–53.
[2] H. Bauer, W. Stelzhammer, R. Fuchs, T. Weiger, C. Danninger, G. Probst, I. Krizbai, Astrocytes and neurons express the tight junction-specific protein occludin *in vitro*, Exp. Cell Res. 250 (1999) 434–438.
[3] H. Braak, I. Alafuzoff, T. Arzberger, H. Kretaschmar, K. del Tredici, Staging of Alzheimer disease-associated neurofibrillary pathology using paraffin sections and immunocytochemistry, Acta Neuropathol. 112 (2006) 389–404.
[4] H. Braak, E. Braak, Neuropathological stageing of Alzheimer-related changes, Acta Neuropathol. 82 (1991) 239–259.
[5] W. Brown, C. Thore, Cerebral microvascular pathology in ageing and neurodegeneration, Neuropathol. Appl. Neurobiol. 37 (2011) 56–74.
[6] L. Dallasta, L. Pisarov, J. Esplen, J. Werley, A. Moses, J. Nelson, C. Achim, Blood–brain barrier tight junction disruption in human immunodeficiency virus-1 encephalitis, Am. J. Pathol. 155 (1999) 1915–1927.

[7] A. Farrall, J. Wardlaw, Blood–brain barrier: ageing and microvascular disease: systematic review and meta-analysis, Neurobiol. Aging 30 (2009) 337–352.

[8] F. Gonzalez-Velasquez, J. Kotarek, M. Moss, Soluble aggregates of the amyloid-β protein selectively stimulate permeability in human brain microvascular endothelial monolayers, J. Neurochem. 107 (2008) 466–477.

[9] S. Hamm, B. Dehouck, J. Kraus, K. Wolburg-Buchholz, H. Wolburg, W. Risau, R. Cecchelli, B. Engelhardt, M.-P. Dehouck, Astrocyte mediated modulation of blood–brain barrier permeability does not correlate with a loss of tight junction proteins from the cellular contacts, Cell Tissue Res. 315 (2004) 157–166.

[10] A. Howarth, M. Hughes, B. Stevenson, Detection of the tight junction-associated protein ZO-1 in astrocytes and other nonepithelial cell types, J. Physiol. 262 (1992) C461–C469.

[11] J. Kirk, J. Plumb, M. Mirakhur, S. McQuaid, Tight junctional abnormality in multiple sclerosis white matter affects all calibres of vessel and is associated with blood–brain barrier leakage and active demyelination, J. Pathol. 201 (2003) 319–327.

[12] I. Krizbai, H. Bauer, N. Bresgen, P. Eckl, A. Farkas, E. Szatmari, A. Traweger, K. Wejksza, H.-C. Bauer, Effect of oxidative stress on the junctional proteins of culture cerebral endothelial cells, Cell. Mol. Neurobiol. 25 (2005) 129–139.

[13] S. Leech, J. Kirk, J. Plumb, S. McQuaid, Persistent endothelial abnormalities and blood–brain barrier leak in primary and secondary progressive multiple sclerosis, Neuropathol. Appl. Neurobiol. 33 (2007) 86–98.

[14] E. Loberg, B. Karlsson, A. Torvik, Neuronal uptake of plasma proteins after transient cerebral ischemia/hypoxia. Immunohistochemical studies on experimental animals and human brains, APMIS 101 (1993) 777–783.

[15] D. Mann, N. Eaves, B. Marcyniuk, P. Yates, Quantitative changes in cerebral cortical microvasculature in ageing and dementia, Neurobiol. Aging 7 (1986) 321–330.

[16] F. Matthews, C. Brayne, J. Lowe, I. McKeith, S. Wharton, P. Ince, Epidemiological pathology of dementia: attributable-risks at death in the MRC cognitive function and ageing study, PLOS Med 6 (2009) e1000180, doi:1000110.1001371/journal.pmed.1000180.

[17] S. Mirra, A. Heyman, D. McKeel, S. Sumi, B. Crain, L. Brownlee, F. Vogel, J. Hughes, G. Van Belle, L. Berg, The consortium to establish a registry for Alzheimer's disease (CERAD). Part II. Standardisation of the neuropathologic assessment of Alzheimer's disease, Neurology 41 (1991) 479–486.

[18] MRC-CFAS, Pathological correlates of late-onset dementia in a multicentre, community-based population in England and Wales, Lancet 357 (2001) 169–175.

[19] S. Nag, A. Kapadia, D. Stewart, Review: molecular pathogenesis of blood–brain barrier breakdown in acute brain injury, Neuropathol. Appl. Neurobiol. 37 (2011) 3–23.

[20] A. Nunomura, R. Castellani, X. Zhu, P. Moreira, G. Perry, M. Smith, Involvement of oxidative stress in Alzheimer disease, J. Neuropathol. Exp. Neurol. 65 (2006) 631–641.

[21] A. Nunomura, T. Hofer, P. Moreira, R. Castellani, M. Smith, G. Perry, RNA oxidation in Alzheimer disease and related neurodegenerative disorders, Acta Neuropathol 118 (2009) 151–166.

[22] A. Nunomura, G. Perry, G. Aliev, K. Hirai, A. Takeda, E. Balraj, P. Jones, H. Ghanbari, T. Wataya, S. Shimohama, S. Chiba, C. Atwood, R. Petersen, M. Smith, Oxidative damage is the earliest event in Alzheimer disease, J. Neuropathol. Exp. Neurol. 60 (2001) 759–767.

[23] M. Penes, X. Li, J. Nagy, Expression of zonula occludens-1 (ZO-1) and the transcription factor ZO-1-associated nucleic acid-binding protein (ZONAB)-MsY3 in glial cells and co-localisation at oligodendrocyte and astrocyte gap junctions in mouse brain, Eur. J. Neurosci. 22 (2005) 404–418.

[24] B. Popescu, E. Toescu, L.M. Popescu, O. Bajenaru, D. Muresanu, M. Schultzberg, N. Bogdanovic, Blood–brain barrier alterations in ageing and dementia, J. Neurol. Sci. 283 (2009) 99–106.

[25] M. Romanitan, B. Popescu, B. Winblad, O. Bajenaru, N. Bogdanovic, Occludin is overexpressed in Alzheimer's disease and vascular dementia, J. Cell. Mol. Med. 11 (2007) 569–579.

[26] K. Sandoval, K. Witt, Blood–brain barrier tight junction permeability and ischemic stroke, Neurobiol. Dis. 32 (2008) 200–219.

[27] J. Simpson, P. Ince, L. Haynes, R. Theaker, C. Gelsthorpe, L. Baxter, G. Forster, G. Lace, P. Shaw, F. Matthews, G. Savva, C. Brayne, S. Wharton, Population variation in oxidative stress and astrocyte DNA damage in relation to Alzheimer-type pathology in the ageing brain, Neuropathol. Appl. Neurobiol. 36 (2010) 25–40.

[28] J. Simpson, P. Ince, G. Lace, G. Forster, P. Shaw, F. Matthews, G. Savva, C. Brayne, S. Wharton, Astrocyte phenotype in relation to Alzheimer-type pathology in the ageing brain, Neurobiol. Aging 31 (2010) 578–590.

[29] J. Simpson, S. Wharton, J. Cooper, C. Gelsthorpe, L. Baxter, G. Forster, P. Shaw, G. Savva, F. Matthews, C. Brayne, P. Ince, Alterations of the blood–brain barrier in cerebral white matter lesions in the ageing brain, Neurosci. Lett. 486 (2010) 246–251.

[30] J.E. Simpson, M. Fernando, L. Clark, P. Ince, F. Matthews, G. Forster, J. O'Brien, R. Barber, R. Kalaria, C. Brayne, P. Shaw, C. Lewis, S. Wharton, White matter lesions in an unselected cohort of the elderly: astrocytic, microglial and oligodendrocyte precursor cell responses, Neuropathol. Appl. Neurobiol. 33 (2007) 410–419.

[31] J. Starr, A. Farrall, P. Armitage, B. McGurn, J. Wardlaw, Blood–brain barrier permeability in Alzheimer's disease: a case–control MRI study, Psychiatr. Res. Neuroimaging 171 (2009) 232–241.

[32] M. Ujiie, D. Dickstein, D. Carlow, W. Jefferies, Blood–brain barrier permeability precedes senile plaque formation in an Alzheimer disease model, Microcirculation 10 (2003) 463–470.

[33] N. Weiss, F. Miller, S. Cazaubon, P.-O. Couraud, The blood–brain barrier in brain homeostasis and neurological diseases, Biochim. Biophys. Acta 1788 (2009) 842–857.

[34] B. Zipser, C. Johanson, L. Gonzalez, T. Berzin, R. Tavares, C. Hulette, V. Hovanesian, E. Stopa, Microvascular injury and blood–brain barrier leakage in Alzheimer's disease, Neurobiol. Aging 28 (2007) 977–986.

[35] B. Zlokovic, The blood–brain barrier in health and chronic neurodegenerative disorders, Neuron 57 (2008) 178–201.